ASPS Conference Proceedings 1: 1441-1447 (2022)

Proceedings of

12th Structural Engineering Convention-An International Event (SEC 2022)

Available at https://asps-journals.com/index.php/acp

Strength of Cold-Formed Stainless-Steel Corrugated Rectangular Sections under Compression

Megha Anto [1, *], Raghavan Ramalingam [1], Jayabalan Perumalsamy [1]

[1] Department of Civil Engineering, National Institute Technology, Tiruchirappalli, 620 015, India

Paper ID - 130349

Abstract

Provision of intermediate stiffening is an effective method to improve the strength of cold-formed steel compression members without having to increase the outer dimensions of the section. As cold-formed sections can be easily produced in various cross-section profiles, the effect of intermediate stiffening on ultimate load carrying capacity and behavior of structural elements need to be determined. In this study columns with Cold-Formed Stainless-Steel and Corrugated Rectangular Hollow Sections are studied numerically using Finite Element analysis. The column simulation is conducted using ABAQUS software including material nonlinearity and performed with the Static Riks procedure. The objective is to study how providing stiffening in the form of corrugations influences the buckling behavior of these columns. Columns for a range of slenderness ratio with varying cross-section parameters were modelled and compared to identify the influencing parameters. The study showed that buckling strength of columns can be significantly increased by providing corrugations. Corrugations effectively resisted local buckling in columns even with low slenderness ratio. The parameters influencing the buckling behavior are identified as cross-section aspect ratio, corrugation height, corrugation width and minimum radius of gyration of the cross-section. Buckling curves are placed for the corrugated sections based on the numerical analysis, and in relation to the buckling curves provided in design standards. On comparing them with the predictions by Euro Code (EN 1993-1-4 (2006)), it was observed that Euro Code predictions are conservative, which is also seen from the buckling curves shown for the corrugated sections.

Keywords: Cold-formed, Stainless-steel, Corrugated sections, Finite element analysis, buckling behaviour

1. Introduction

Stainless-steel with its high corrosion resistance has gathered wide acceptance as a structural material in the recent years. Because of its excellent cold forming properties, stainless steel is cheaper to work with. The basic material stress-strain curve of stainless-steel is one of the unique features that makes it different carbon steel [1]. Stainless steel has greater strength and work hardening than carbon steel. This is why cold-formed stainless steel tubular members are widely used these days for construction, as truss girders, columns in framed structures, members in roof structures and so on. In most of the cases they are used as compression members. While using cold-formed stainless-steel hollow compression members are itself advantageous, giving a corrugated profile can be expected to further increase the strength without having to provide external reinforcement [2]. Corrugations provide intermediate stiffening which permits the use of slender elements. Hence corrugated member can prove to be more cost effective than conventional hollow members. There are design

There are test carried out on cold-formed stainless-steel hollow square and rectangular columns stating that the design strengths predicted by American (ASCE 1991), Australian/New Zealand (Aust/NZS 2001), and European specifications available for Cold-formed stainless-steel structural elements such as the American (ASCE 1991) [3], Australian/ New Zealand (Aust/NZS 2001) [4], and European (Eurocode 3 1996) specifications [5-8] for cold-formed stainless steel structures. But these specifications do not contain information on the behaviour of sections with corrugated stiffening. Cold-formed steel columns having different cross-sectional shapes have been studied by various researchers [9,10]. But there are a very few studies carried out on corrugated sections under compression. Over the recent years a few different types of innovative columns have been the topic of study with an aim to economically improve the axial load capacity of columns [11,12]. Recently, Nassirnia et al carried out tests on innovative mild steel column showing the higher load carrying capacity of corrugated profiles than rectangular hollow cold-formed steel section [13]. Narayanan and Mahendran investigated the distortional buckling behaviour of innovative cold-formed steel columns taking into account the effect of geometric imperfections and residual stresses [14]. (Eurocode 3 1996) are conservative [15-18]. The finite element model developed by Ellobody and Young is accurate and effective in predicting the behaviour of cold-formed high strength stainless steel columns [19]. Residual

*Corresponding author. Tel: +919633202742; E-mail address: meghaanto@gmail.com

Published online: December 19, 2022

doi:10.38208/acp.v1.674

stresses, especially membrane residual stresses are proven to be higher in cold-formed stainless steel sections as compared to hot-rolled sections. But their influence in the analysis is low and can be neglected in most cases [20,21]. It is imperative to incorporate geometric non-linearity in buckling analysis. Various recent studies shows different approaches to incorporate geometric imperfections in the analysis of cold-formed steel members [22-24].

In this study a series of cold-formed stainless steel corrugated rectangular columns is numerically studied by varying different cross-section geometric properties namely aspect ratio, height of corrugation and corrugation width to side width ratios. Based on the negligible influence of residual stresses, only geometric imperfections are included.

2. Finite Element Modelling and Validation

Finite element model was developed and analysed using ABAQUS software [13]. The models are validated with the specimens tested experimentally by Young and Liu [15]. A specimen was chosen from the series R1 with material properties obtained from tensile coupon test as specified in Table 1. The cross-sectional parameters of this specimen is given in Table 2.

Residual stress due to cold working is ignored in this study. The stress-strain curve of the material is included in the finite element model to incorporate material non-linearity [15]. The element type chosen for the model is S4R. Geometric imperfection is considered as a linear superposition of buckling Eigen modes. The imperfection factor is adopted based on the study by Schafer et al [22]. A factor of 50% is used, considered with values of 0.34t for local imperfections. A value of L/1500 is used for overall Buckling imperfection, where L is the length of column. Fixed-Fixed boundary condition is adopted for the model as

in the test setup. It is ensured that both the load carrying capacity and the behaviour of the specimens in the inelastic region is also matched to a good extent. Fixed-fixed boundary condition is adopted for the model as in the test setup [15]. Table 3 shows the comparison of buckling loads obtained from Finite-element analysis and experimental test.

The column R1L2000 failed through a local-global interactive buckling. The failure patterns in FE models were similar to the failure modes observed in the experiment

Table-1 Material Properties from coupon test

Eo (Gpa)	$\sigma_{0.2}$ (Mpa)	$\sigma_{0.5}$ (Mpa)	σ_u (Mpa)	ε_u (Mpa)
198	350	381	649	72%

Table-2 Cross-section properties

Depth (D)	Width (B)	Thickness (t)	Area (A)
120 mm	40 mm	2 mm	595 mm^2

Table 3 Comparison of FE analysis results with experimental results

Specimen	Length (mm)	Experimental Buckling Load	FEM Buckling Load	Percentage Variation (%)
R1L2000	2000	141.30	148.83	5.3

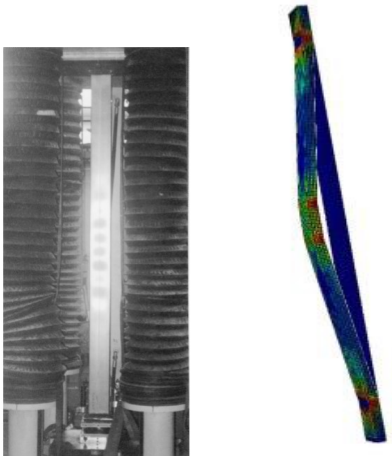

(a) (b)

Fig 1 Failure of R1L2000 under combined local and overall flexural buckling: (a) Test specimen [15], (b) Numerical model

3. Parametric study

The material properties adopted for all the models in this study correspond to the material properties of series R1 used in the experimental investigation by Young and Liu [15], and used for validation of the numerical model. In the current study different series of cross-sections are considered. In Parametric Study-I, two rectangular hollow sections having different aspect ratios (D/B) is considered. In Parametric Studies-II to IV, different corrugated sections having varying corrugation parameters are considered along with a control section, keeping the cross-section area constant for every section. The corrugation angle is kept constant as 90° for all the corrugated sections. The corrugated profile is such that two opposite sides are flat, while the other two sides have corrugations with three crest panels and two trough panels each. The control section is a rectangular hollow CFS section. Columns having different slenderness ratios are modelled for each of these sections by varying the length of column. Thus, each series of columns consists of columns with the same cross-section, having varying lengths.

3.1 Parametric Study-I: Rectangular section -Varying D/B, Keeping t constant

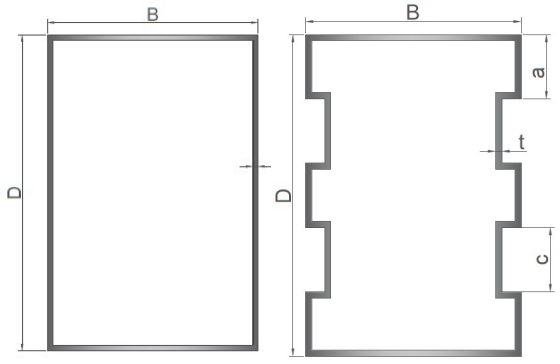

Fig 2 Rectangular and corrugated sections

Here, two rectangular sections C1 and C2 having different aspect ratio (D/B) are considered [15]. The cross-sectional parameters are given in Table 4. B is the width of the section, D is the overall depth, a is the corrugation width, t is the thickness and R_y is the minimum radius of gyration of the section.

Table 4 Section Properties for C1 and C2

Series	Depth D (mm)	Width B (mm)	Thickness t (mm)	R_y (mm)	Area A (mm^2)
C1	120	40	2	18.16	595
C2	120	80	2	34.32	1520

Table 5 shows the failure loads obtained from Non- Linear Finite Element analysis of these sections for different lengths. Here 10 columns having varying lengths are considered for each of the series. Slenderness ratio (kL/R_y) varied from a minimum of 40 to 200.

Figure 3 shows the buckling curve plotted for C1 and C2 based on Euro Code method, where χ is the reduction factor to be used with the strength of effective section to get the failure load and λ' is the non-dimensional slenderness ratio.

In series C1, C1L1200 (column with length 1200mm in series C1) failed under local buckling, while C1L1500 and C1L2000 failed under local-global interactive buckling. The remaining columns failed by global buckling. In series C2, columns C2L2000 to C2L4000 failed under local buckling. C2L5000 and C2L6000 failed under local-global interactive buckling. The remaining failed by global buckling. Clearly, global buckling is delayed in series C2. For the same length of column, columns in series C1 has higher slenderness ratio compared to that in series C2. Also, from Figure 5, for the same value of non-dimensional slenderness ratio, C2 has higher reduction factor compared to C1. This shows that sections with higher aspect ratio is more effective in resisting compression.

Table 5 Buckling load for C1 and C2

C1			C2		
Length	kL/R_y	Load (KN)	Length	kL/R_y	Load (KN)
1200	43.89	166.2	2000	37.88	195.63
1500	54.87	165.8	3000	56.82	195.57
2000	73.16	139.89	4000	75.76	195.52
2500	91.45	136.64	5000	94.70	195.38
3000	109.7	118.6	6000	113.64	195.36
4000	146.3	89.81	7000	132.58	192.42
4500	164.6	75.2	8000	151.52	169.18
5000	182.9	59.87	9000	170.45	130.27
5500	201.2	49.2	10000	189.39	101.29
6000	219.5	43.32	11000	208.33	81.40

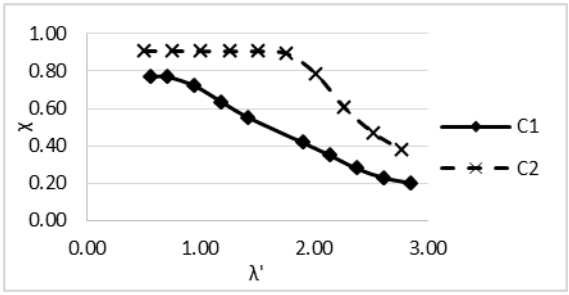

Fig 3 Buckling Curve for series C1 and C2

3.2 Parametric Study-II: Corrugated section-Varying h, keeping D/B constant

Here three corrugated sections are considered along with the control section. Corrugated sections are formed by varying corrugation height, while keeping the cross-sectional area and D/B as same as that of the control section [13]. a/D ratio for all the three sections are kept as 0.2. Table 6 shows the cross-section properties of the sections considered in this study. Here h is the corrugation Height.

Table 6 Section Properties for C1, C1H5, C1H8, C1H10

(D/B=3, Area=624mm^2, a/D= 0.2)

Series	B(mm)	D(mm)	a(mm)	t(mm)	h(mm)	R_y
C1	40	120	24	2	0	18.17
C1H5	35	105	21	2	5	14.05
C1H8	32	96	19.2	2	8	11.65
C1H10	30	90	18	2	10	10.27

The Tables 7 and 8 show the results obtained from non-linear static analysis for different columns heights every series. It was observed that beyond a slenderness-ratio of 150 the effect of corrugation is not significant. Hence, 6 columns are considered in every series between a range of slenderness-ratio of 50-150.

Table 7 Buckling load for C1H5

C1H5		
Length	kL/Ry	Load (KN)
1200	55.52	211.6
1500	69.40	207.9
2000	92.53	185.6
2500	115.66	146.4
3000	138.79	100.6
3500	161.92	79.58

Table 8 Buckling load for C1H8 and C1H10

C1H8			C1H10		
Length	kL/Ry	Load (KN)	Length	kL/Ry	Load (KN)
1000	55.79	210.90	1000	63.28	201.92
1250	69.74	205.91	1250	79.10	195.60
1500	83.69	194.41	1500	94.92	176.44
2000	111.59	153.48	1750	110.74	142.77
2500	139.48	106.19	2000	126.56	123.43
3000	167.38	76.76	2500	158.20	85.49

It was expected that for the same length of column and same cross-sectional area, buckling strength would increase with increase in corrugation height (h) [5]. But the results showed otherwise. When corrugation height is increased while keeping the aspect ratio (D/B) same, the R_y value decreases. Thus, for columns of same length, slenderness ratio will be more for the one with higher corrugation height. So the increase in stiffness due to higher corrugation height is compensated by the increased instability due to higher slenderness ratio, as observed from the results

3.3 Parametric Study-III: Corrugated section-Varying D/B

Another series was modelled by keeping R_y as same as that of C1H5, with corrugation height (h) as 8mm by varying the D/B ratio. Here C1H5 and C1H8-A have almost the same value of R_y but different h, whereas C1H8 and C1H8-A have the same h but different R_y. Table 11 shows the buckling loads for the section C1H8-A for different lengths. It was observed that when corrugation height (h) is increased for

Table 10 Section Properties for C1H5, C1H8, C1H8-A

(Area=624mm^2, a/D= 0.2, t= 2mm)

Series	B(mm)	D(mm)	a(mm)	h(mm)	D/B	Ry
C1H5	35	105	21	5	3	14.05
C1H8	32	96	19.2	8	3	11.65
C1H8-A	38	90	18	8	2.37	13.95

Table 11 Buckling load for C1H8-A

C1H8-A		
Length	kL/Ry	Load (KN)
1200	55.91	219.62
1500	69.89	211.57
2000	93.19	196.54
2500	116.49	161.42
3000	139.78	122.47
3500	163.08	93.02

the same length of column while keeping R_y constant, buckling strength increases. Also when R_y is increased keeping h constant, buckling strength increases. C1H8-A has higher buckling strength than both C1H5 and C1H8. C1H8-A has both higher corrugation height as well as R_y value. C1H8-A has higher buckling strength than both C1H5 and C1H8. C1H8-A has both higher corrugation height as well as R_y value.

3.4 Parametric Study-IV: Corrugated section-Varying a/D, keeping h constant

In this parametric study a/D ratio was varied by changing corrugation width (a), while keeping the corrugation height (h) constant. C1H8-A which showed better strength in the earlier studies had a/D value 0.2. 2 more sections with a/D ratio 0.1 and 0.3 were considered for this comparison. It should be noted that when 'a' is maximum**,** 'c 'is minimum.

Table 12 Section Properties for C1H8-A, C1H8-B, C1H8-C

(Area=624mm2, D/B=2.37, t= 2mm, h= 8mm)						
Series	B(mm)	D(mm)	a(mm)	c(mm)	a/D	Ry
C1H8-A	38	90	18	18	0.2	13.95
C1H8-B	38	90	9	31.5	0.1	12.16
C1H8-C	38	90	27	4.5	0.3	14.50

Table 13 Buckling load for C1H8-C

C1H8-C		
Length	kL/Ry	Load (KN)
1250	56.04	219.41
1500	67.25	216.26
2000	89.66	205.46
2500	112.08	178.32
3000	134.49	139.13
3500	156.91	111.26

Comparison of columns with height 2500 in all the three sections showed that the column with maximum a/D ratio showed better performance. As the corrugation height (a) is increased, R_y value increases and hence the slenderness ratio decreases for the same length of column. This explains why C1H8-B has the lowest strength for the same height of column. Therefore, no further study was carried out on C1H8-B.

Table 14 and Figure 4 shows the comparison of buckling loads for columns with height 2500mm for different cross-section to have a better glimpse at the change in buckling behaviour of columns with change in cross-sectional parameters. Clearly, C1H8-C showed better buckling behaviour compared to all the other sections. It is the section with maximum corrugation height, maximum value of minimum radius of gyration, as-well as maximum a/D ratio.

Table 14 Buckling load for columns with height 2500mm

Series	kL/ Ry	Load(KN)	Ry
C1	89.43	136.64	18.17
C1H5	115.66	150.21	14.05
C1H8	139.48	106.19	11.65
C1H10	158.20	85.49	10.27
C1H8-A	116.49	161.42	13.95
C1H8-B	113.62	139.57	12.16
C1H8-C	112.08	178.32	14.5

Figure 5 shows the buckling curve plotted for all the corrugated columns along with the buckling curve of Series

C1. It can be seen that the buckling curves of all the corrugated sections nearly coincides .Which indicates that they have similar buckling behaviour. Clearly more portion of the cross-section is effective in corrugated columns which results in higher load carrying capacity compared to conventional rectangular columns.

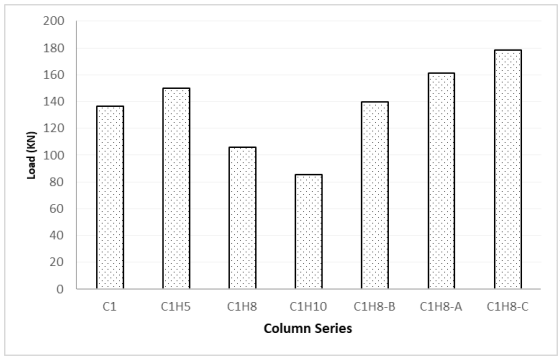

Fig. 4 Comparison of buckling load for columns with height 2500mm

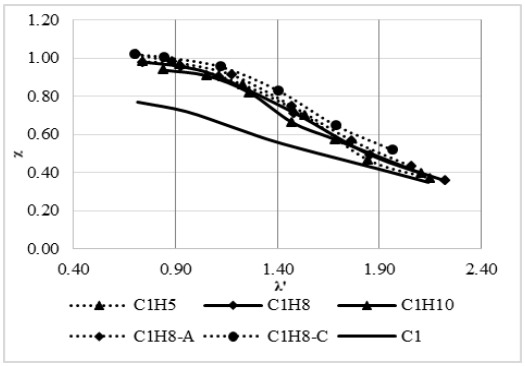

Fig 5 Buckling Curve for Rectangular and Corrugated sections

4. Failure modes in corrugated columns

The prominent mode of failure in corrugated columns within the range of slenderness ratio 50-150 was observed to be global buckling, while a few columns with low slenderness ratio exhibited local-global interactive buckling. In the series C1 columns with lengths 1500 and 2000 showed local-global interactive buckling, while all the other with higher slenderness ratio failed under global buckling. Considering that in the series of corrugated sections, the columns with length 1500 and 2000 exhibited global buckling behaviour, it can be concluded that providing corrugations has effectively resisted local buckling in columns. Figure 6 shows the deformed shape of Column with a height of 2500mm from the series C1H8-C.

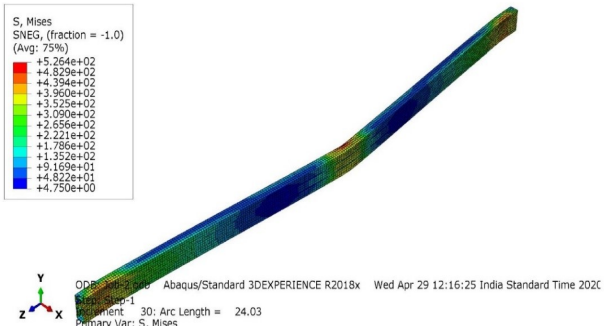

Fig 6 Deformed shape of column with height 2500mm in C1H8-C

5. Comparison of Euro code predictions to corrugated sections

Buckling curves were plotted for all the corrugated sections considered in the study from buckling load proposed by Euro code (EN 1993-1-4 (2006)) [7] as well as that obtained from numerical analysis. Here λ' is the non-dimensional slenderness ratio. P_{EN} and P_{num} are the buckling loads obtained from Euro code and numerical analysis respectively. χ_{EN} and χ_{num} are the reduction factors obtained from Euro-code and numerical analysis respectively. Partial factors were removed from the calculations in order to obtain the ultimate values. Tables 15 to 19 shows the comparison of Euro-code predicted buckling load with that obtained from simulation.

Fig 7 shows the comparison of buckling curves of the corrugated sections considered in the study in relation to the buckling curves present in Euro-Code. In all of the sections the buckling curve shows that the Euro code prediction is very much conservative. Also, the form of the curve predicted by the Euro code is also different. In the Euro code buckling curve, the rate of fall in failure load with increase in non-dimensionless slenderness ratio is rapid initially and then slows down at higher slenderness ratio. Whereas in the numerical curve the rate is slow initially and then it increase at higher slenderness ratio. All the buckling curve for all the sections plotted from the numerical obtained values follows the same trend. As λ' varies from around 0.70 to 2.00, PEN/Pnum varies from around 0.75 to 4.00. All the buckling curves obtained from the numerical analysis of different corrugated sections were overlapped and a curve which best fits the general behaviour was drawn. Figure 8 shows this curve along with the buckling curve proposed by Euro-code.

Table 15 Ultimate Load From Euro Code for C1H5

Length	λ'	P_{EN}	χ_{EN}	P_{num}	χ_{num}	P_{EN}/P_{num}
1200	0.74	167.64	0.78	211.60	0.98	0.79
1500	0.92	138.17	0.64	207.91	0.96	0.66
2000	1.23	96.16	0.45	185.61	0.86	0.52
2500	1.54	67.99	0.32	150.21	0.70	0.45
3000	1.84	49.95	0.23	100.62	0.47	0.50
3500	2.15	38.07	0.18	79.58	0.37	0.48

Table 16 Ultimate Load From Euro Code for C1H8

Length	λ'	P_{EN}	χ_{EN}	P_{num}	χ_{num}	P_{EN}/P_{num}
1000	0.74	166.89	0.77	210.90	0.98	0.79
1250	0.93	137.24	0.64	205.91	0.96	0.67
1500	1.11	110.35	0.51	194.41	0.90	0.57
2000	1.48	71.91	0.33	153.48	0.71	0.47
2500	1.85	49.40	0.23	106.19	0.49	0.47
3000	2.23	35.78	0.17	76.76	0.36	0.47

Table 17 Ultimate Load From Euro Code for C1H10

Length	λ'	P_{EN}	χ_{EN}	P_{num}	χ_{num}	P_{EN}/P_{num}
1000	0.84	150.88	0.70	201.92	0.94	0.75
1250	1.05	118.65	0.55	195.60	0.91	0.61
1500	1.26	92.41	0.43	176.44	0.82	0.52
1750	1.47	72.78	0.34	142.77	0.66	0.51
2000	1.68	58.35	0.27	123.43	0.57	0.47
2500	2.10	39.57	0.18	85.49	0.40	0.46

Table 18 Ultimate Load From Euro Code for C1H8-A

Length	λ'	P_{EN}	χ_{EN}	P_{num}	χ_{num}	P_{EN}/P_{num}
1200	0.71	172.63	0.80	219.62	1.02	0.79
1500	0.88	144.41	0.67	211.57	0.98	0.68
2000	1.18	102.35	0.47	196.54	0.91	0.52
2500	1.47	73.01	0.34	161.42	0.75	0.45
3000	1.76	53.87	0.25	122.47	0.57	0.44
3500	2.06	41.16	0.19	93.02	0.43	0.44

Table 19 Ultimate Load From Euro Code for C1H8-C

Length	λ'	P_{EN}	χ_{EN}	P_{num}	χ_{num}	P_{EN}/P_{num}
1250	0.70	172.97	0.80	219.41	1.02	0.79
1500	0.84	150.48	0.70	216.26	1.00	0.70
2000	1.13	108.70	0.50	205.46	0.95	0.53
2500	1.41	78.30	0.36	178.32	0.83	0.44
3000	1.69	58.06	0.27	139.13	0.65	0.42
3500	1.97	44.48	0.21	111.26	0.52	0.40

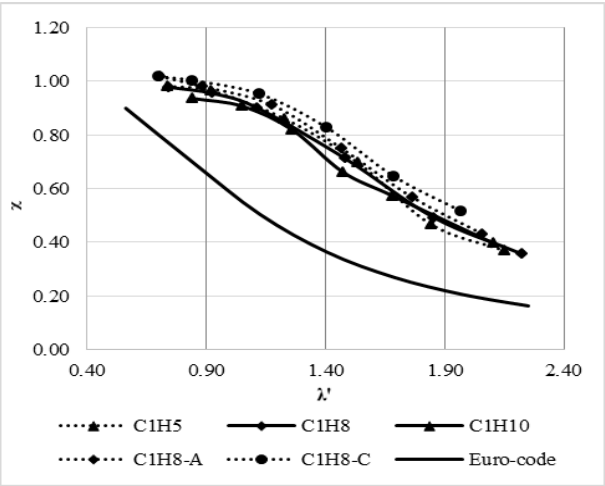

Fig 7 Buckling Curve for corrugated sections

Clearly Euro-code does not accurately predict the behaviour of Cold-formed corrugated sections. With a more elaborate study considering more parameters such as thickness of the section, material properties etc., it could be possible to suggest a new curve or a set of buckling curves for corrugated section.

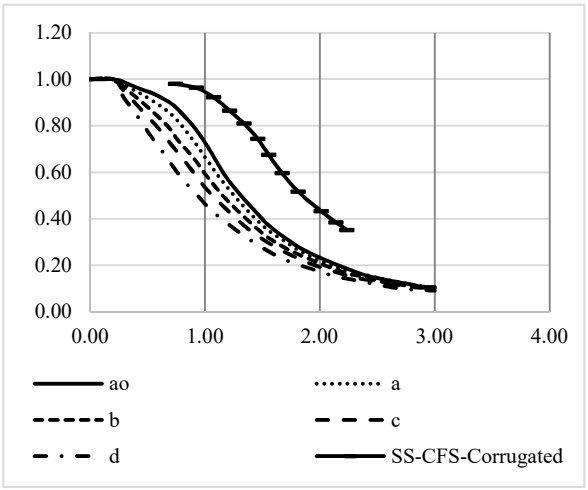

Fig 8 Buckling Curves

6. Conclusions

This paper discussed the behaviour of cold-formed steel rectangular and corrugated sections under compression. A detailed parametric study has been done using finite-element analysis with a numerical model developed using experimental results available in literature. A review on the applicability of Euro code predictions on cold-formed stainless steel corrugated sections under compression has also been presented. Based on these studies several conclusions are derived below.

1. In rectangular sections with higher D/B ratio overall buckling is delayed with respect to slenderness ratio. These sections are more effective in resisting compression than the sections with lesser D/B ratio. Buckling strength of these CFS columns can be enhanced by providing corrugations
2. Strength of a corrugated columns can be improved for the same amount of material by shaping a cross-section such that it has
    a. Maximum corrugation height (h)
    b. Maximum value of minimum Radius of Gyration of the section (R_y)
    c. Maximum a/D ratio
3. Local buckling is effectively resisted by providing corrugations, though the effect of corrugations is negligible beyond a slenderness-ratio 150
4. The existing code predications under-estimates the strength and does not accurately predict the buckling behaviour of cold-formed stainless-steel corrugated section
5. Further studies are required to improve the accuracy of code provisions for profiled sections

Disclosures

Free Access to this article is sponsored by SARL ALPHA CRISTO INDUSTRIAL.

References

1. Gardner, L., Nethercot, D. A., (2004), Experiments on stainless steel hollow sections-Part 1: Material and cross-sectional behaviour, Journal of Constructional Steel Research, 60(9), 1291-1318.
2. Liew K. M., Peng L. X. and Kitipornchai S., (2006), Buckling analysis of corrugated plates using a mesh-free Galerkin method based on the first-order shear deformation theory, Computational Mechanics, 38, 61–75
3. American Society of Civil Engineers (ASCE) 8-02, Specification for the Design of Cold-Formed Stainless-Steel Structural Members.
4. Australian/ New Zealand Standard, AS/NZS 4673:2001, Cold-formed stainless steel structures."
5. Eurocode 3 -EN 1993-1-1 (2005), Design of steel structures - Part 1-1: General rules and rules for buildings.
6. Eurocode 3 -EN 1993-1-3 (2006), Design of steel structures - Part 1-3: General rules - Supplementary rules for cold-formed members and sheeting.
7. Eurocode 3 -EN 1993-1-4 (2006), Design of steel structures – Part 1-4: General rules - Supplementary rules for stainless steels.
8. Eurocode 3 -EN 1993-1-5 (2006), Design of steel structures – Part 1-5: General rules – Plated structural elements.
9. Guo L., Yang S. and Jiao H. (2013), Behavior of thin-walled circular hollow section tubes subjected to bending, Thin Walled Structures, 73, 281–289.
10. Zhu J.H. and Young B. (2011), Cold-Formed-Steel Oval Hollow Sections Under Axial Compression, Journal of Structural Engineering, 137(7), 719-727.
11. Nassirnia M., Heidarpour A., Zhao X.L. (2016), Innovative hollow columns comprising corrugated plates and ultra high-strength steel tubes, Thin Walled Structures, 101, 14-25.
12. Javidan F, Heidarpour A., Zhao X.L. (2015), Performance of innovative fabricated long hollow columns under axial compression, Journal of constructional steel research, 106, 99-109.
13. Nassirnia M., Heidarpour A., Zhao X. L. and Minkkinen J. (2015), Innovative hollow corrugated columns: a fundamental study, Engineering structures, 94, 43-53.
14. Narayanan S. and Mahendran M. (2003), Ultimate capacity of innovative cold-formed steel columns. Journal of constructional steel research, 59(4), 489-508.
15. Young B. and Liu Y. (2003), Experimental Investigation of Cold-Formed Stainless Steel Columns, Journal of Structural Engineering, 129(2), 169-176.
16. Young B. and Lui W.M. (2005), Behavior of Cold-Formed High Strength Stainless Steel Sections, Journal of Structural Engineering, 131(11), 1738-1745.
17. Young B. and Lui W.M. Tests of cold-formed high strength stainless steel compression members, (2006), Thin-Walled Structures, 44, 224–234.
18. Bešević M., Prokić A., Landović A. and Kasaš K., (2017), The Analysis of Bearing Capacity of Axially Compressed Cold Formed Steel Members, Periodica Polytechnica Civil Engineering, 61(1), 88–97.
19. Ellobody B. and Young B. (2005), Structural performance of cold-formed high strength stainless steel , Journal of constructional steel research, 61(12), 1631-1649.
20. Cruise R.B. and Gardner L. (2008), Strength enhancements induced during cold forming of stainless steel section, Journal of constructional steel research, 64(11), 1310-1316.
21. Jandera M. and Machacek J. (2014), Residual stress influence on material properties and column behaviour of stainless stell SHS, Thin Walled Structures, 83, 12-18.
22. Schafer B. W. and Peköz T. (1998), Computational modelling of cold-formed steel: characterizing geometric imperfections and residual stresses, Journal of constructional steel research, 47(3), 193-210.
23. Zeinoddini V. M. and Schafer B. W (2012),Simulation of geometric imperfections in cold-formed steel members using spectral representation approach, Thin-Walled Structures 60, 105–117
24. Sadovský Z., Kriváček J., Ivančo V. and Ďuricová A. (2012), Computational modelling of geometric imperfections and buckling strength of cold-formed steel, Journal of Constructional Steel Research 78, 1–7